

H₂/D₂ exchange reaction on mono-disperse Pt clusters: Enhanced activity from minute O₂ concentrations

Jakob Nordheim Riedel, Marian David Rötzer, Mikkel Jørgensen, Ulrik Grønbjerg Vej-Hansen, Thomas Pedersen, Béla Sebök, Florian Frank Schweinberger, Peter Christian Kjærgaard Vesborg, Ole Hansen, Jakob Schiøtz, Ulrich Heiz, and Ib Chorkendorff

Electronic Supplementary Information

Sample Preparation

A mass scan of the cluster beam is shown in figure S1. A clear separation of the peaks proves that the Pt₈ sample is indeed mono-dispersed.

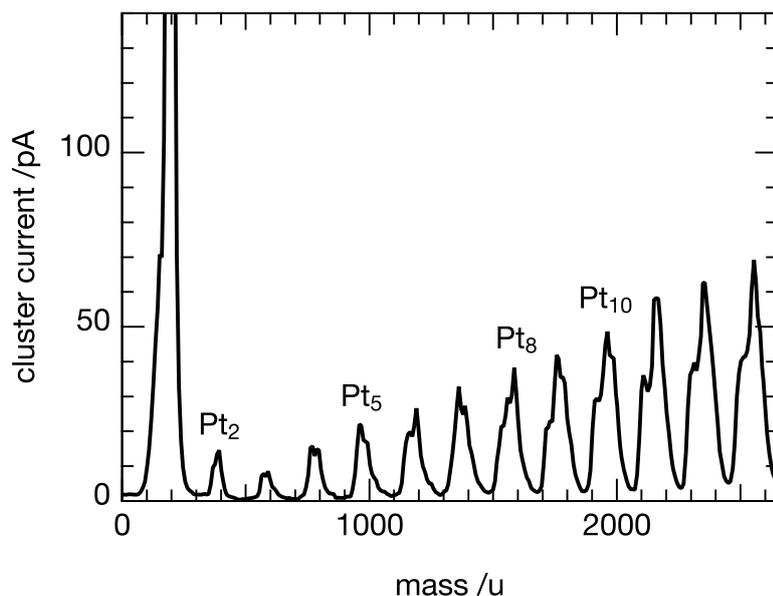


Figure S1: Mass scan of the cluster current. A clear separation of the cluster peaks indicates mono-disperse clusters during deposition.

Characterisation

Spectroscopic characterisation was conducted in a UHV chamber (Omicron NanoTechnology). The chamber is equipped with an X-ray gun (SPECS XR 50 X-ray gun) and a hemispherical analyser (Omicron NanoSAM 7 channel energy analyser) for XPS. An ion gun (Omicron ISE100 ion gun) is fitted for ISS.

ISS

ISS data after chemical testing of the Pt_8 sample is shown in figure S2.

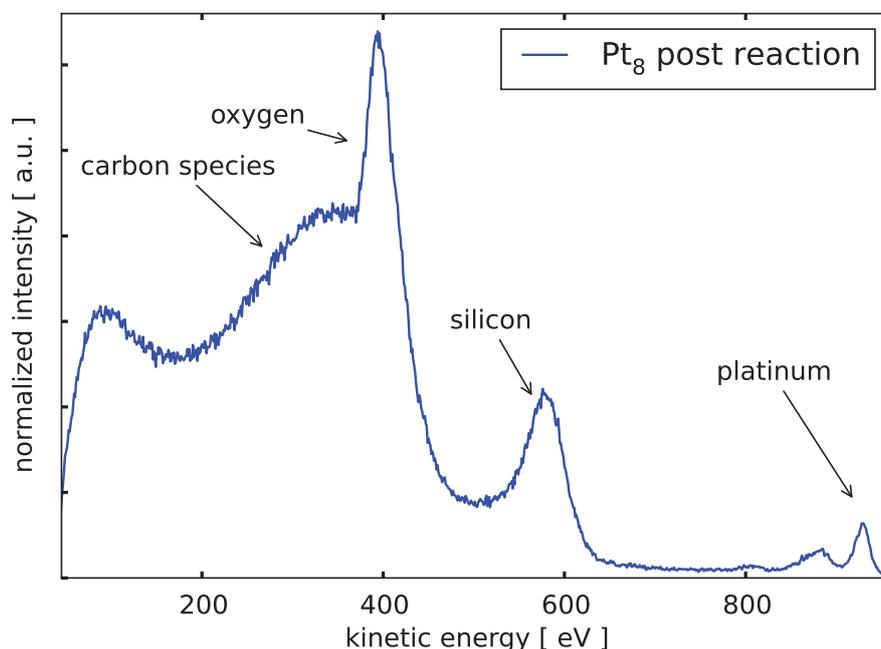


Figure S2: ISS spectra of Pt_8 after chemical activity testing.

XPS

The binding energies of all XPS spectra were shifted to fit the carbon 1s peak at 284.6 eV and normalized to the SiO_2 peaks. All spectra were made with a magnesium anode with a FWHM of 0.7 eV and without a monochromator. Experimental details are shown in table S1.

Figure S3 shows XPS overview scans of the $\text{Pt}_{\geq 8}$ sample before and after chemical testing. Due to a low signal to noise ratio on the platinum 4f doublet, fitted parameters are somewhat uncertain.

Figure S4 shows XPS data of the Pt_8 sample after chemical testing.

Parameters extracted from XPS data in figure 4 of the main article are summarized in table S2.

Table S1: Experimental values for XPS data acquisition.

scan type	scan range [eV]	pass energy [eV]	step size [eV]	scans [#]	dwell time [s]
survey	1050 to -5	50	0.5	2	0.5
detailed	100 to 50	25	0.2	10	0.2

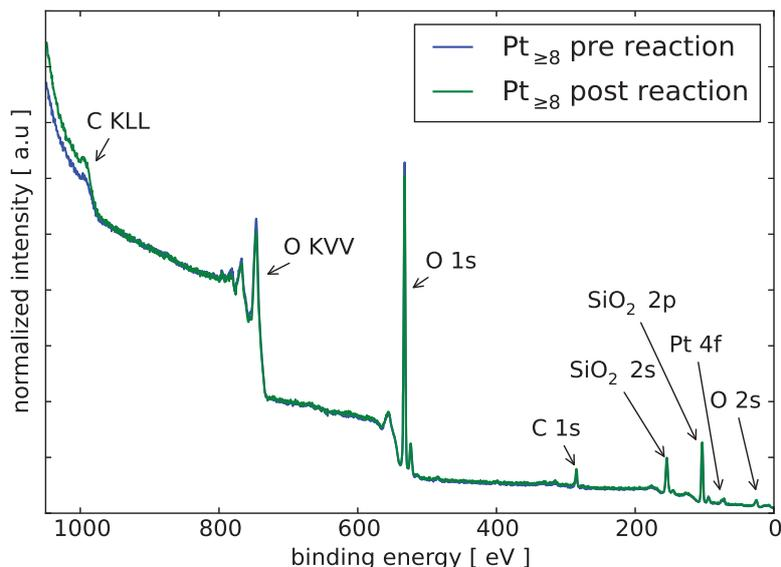


Figure S3: XPS overview spectra of $\text{Pt}_{\geq 8}$ before (blue) and after (green) chemical activity testing.

Chemical activity

Chemical activity data for sample $\text{Pt}_{\geq 8}$ is shown in figure S5. A background proportional to the $m/z = 4$ was subtracted from the $m/z = 3$ signal, resulting in a measure of the HD production. It is not possible to calculate a TOF since the amount of platinum in the reactor is unknown, because the size of the clusters is unknown.

Raw signals from the QMS of reactant masses shown in figure S6. $m/z = 2$ comes from H_2 , $m/z = 4$ is from D_2 , and $m/z = 20$ and $m/z = 40$ is from Ar. All masses decrease with temperature due to the decrease in gas flow through the reactor. The $m/z = 20$ signal is dominated by the Ar dosage and is therefore proportional to the $m/z = 40$ signal.

Masses $m/z = 18$ (H_2O), 19 (HDO), 28 (CO/N_2), 32 (O_2), and 44 (CO_2) are shown in figure S7. All signals are dominated by a permanent offset. The water signal ($m/z = 18$) is constant up to $\sim 120^\circ\text{C}$ where it increases slightly. It is higher than the HDO signal, indicating that it originates from desorption from the system, and to a lesser extent a catalytic reaction between H_2 , D_2 , and O_2 to form water. The $m/z = 28$ signal indicates CO or N_2 . The first could come from dosed O_2 reacting

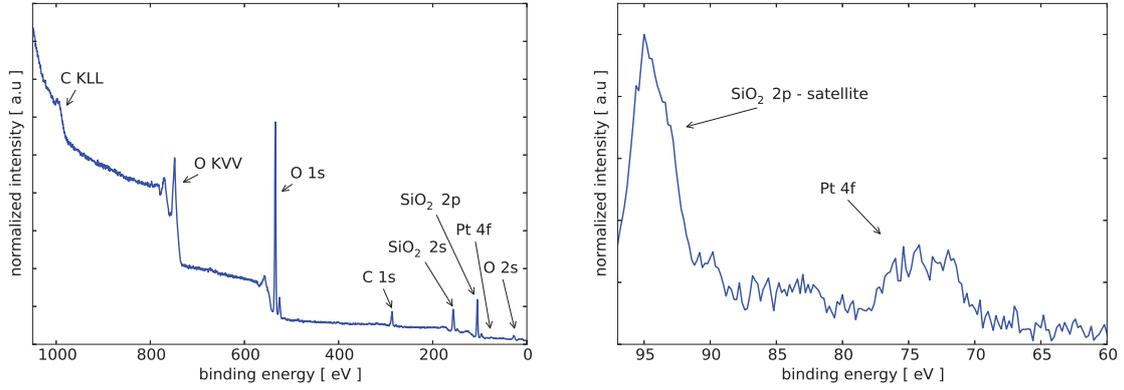


Figure S4: XPS spectra of the Pt_8 sample after chemical testing. Left shows an overview scan. Right shows a zoom in on the SiO_2 satellite peak and the Pt doublet peak.

Table S2: Parameters from a fit to the normalized XPS data in figure 4 in the main article of the $\text{Pt}_{\geq 8}$ sample.

spectrum	peak name	binding energy [eV]	FWHM [eV]	area [a.u.]
pre reaction	Pt $4f_{7/2}$	71.9	2.6	1.38
	Pt $4f_{5/2}$	75.2	2.4	1.04
post reaction	Pt $4f_{7/2}$	71.8	2.8	1.83
	Pt $4f_{5/2}$	75.0	2.7	1.37

with carbon from the filament of the QMS. The latter could come from rubber o-rings leaking at higher temperatures.

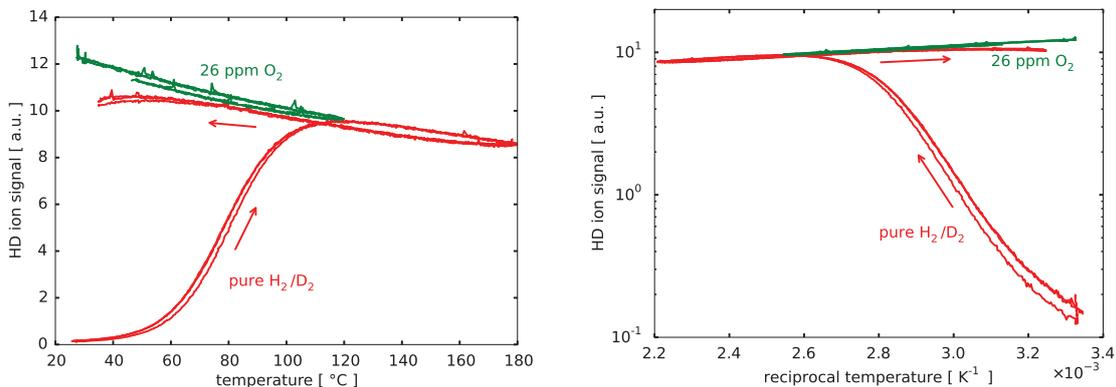


Figure S5: Left shows the HD production as function of temperature from the $\text{Pt}_{\geq 8}$ sample. An Arrhenius plot of the same data is shown on the right.

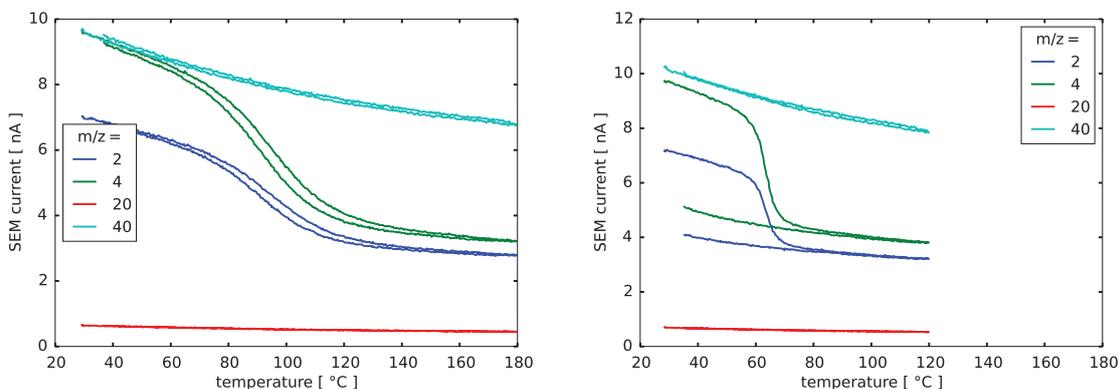


Figure S6: Reactant signals measured during HD production of the Pt_8 sample. Left shows signals during pure H_2/D_2 dosage and right show the same signals while dosing 26 ppm O_2 .

DFT

Figure S8 shows the relaxed atomic configurations of Pt_8 on a SiO_2 support as calculated using DFT.

The binding energies for oxygen on the lowest-energy cluster calculated using DFT are shown in figure S9.

The numbering of sites on the platinum cluster is shown in figure S10.

Calculated activity and desorption energies for hydrogen at various sites on the lowest energy cluster, with and without adsorbed OH, are shown in table S3.

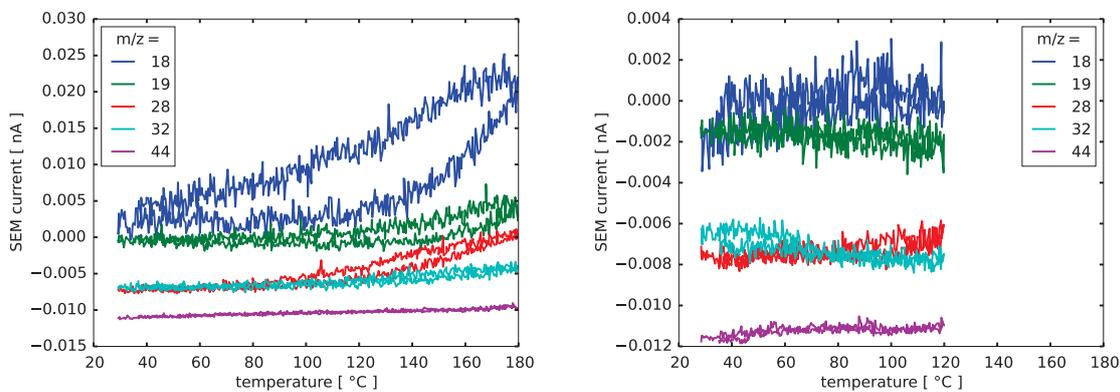


Figure S7: Signals from bi-products measured during HD production of the Pt_8 sample. Left shows signals during pure H_2/D_2 dosage and right show the same signals while dosing 26 ppm O_2 .

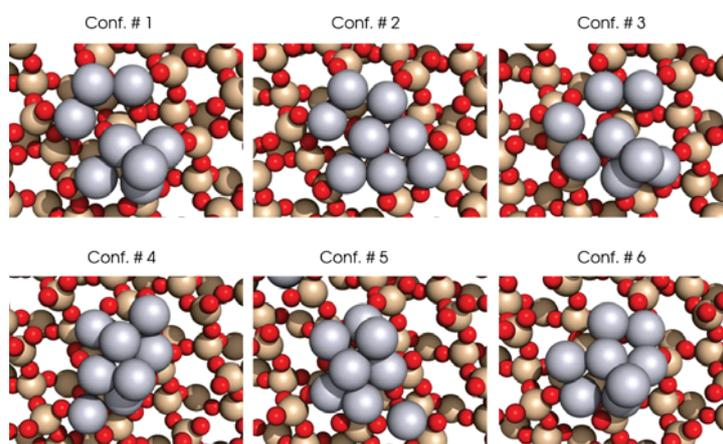


Figure S8: Relaxed atomic configurations ordered by decreasing binding energy. Atoms are color coded; platinum (grey), silicon (golden), and oxygen (red).

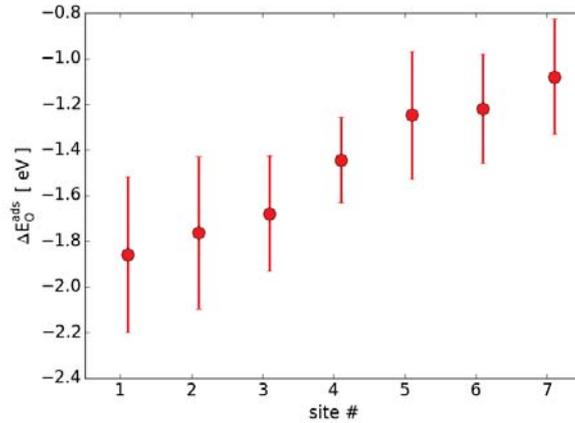


Figure S9: Adsorption energy of oxygen on different sites on the lowest-energy cluster. More negative means stronger binding.

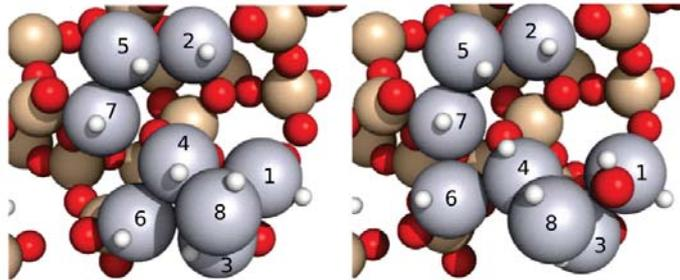


Figure S10: Numbering of atoms in the cluster for determining the site combination used for hydrogen dissociation. Atoms are color coded; platinum (grey), silicon (golden), and oxygen (red).

Table S3: Activation and adsorption energies calculated with DFT for the lowest energy cluster with and without adsorbed OH. $E_{\text{H,Pt}}$ and $E_{\text{H,Pt-OH}}$ denote the dissociative adsorption energy of H_2 without and with oxygen respectively. $\Delta E_{\text{H}} = E_{\text{H,Pt-OH}} - E_{\text{H,Pt}}$ is the difference of these two and ΔA is the resulting change in activity. Dissociation sites on the cluster are shown in figure S10.

sites	$E_{\text{H,Pt}}$ [eV]	$E_{\text{H,Pt-OH}}$ [eV]	ΔE_{H} [eV]	ΔA [s^{-1}]
1-8	-0.13	-0.24	-0.10	-1.1×10^1
1-3	-0.42	0.42	0.84	1.9×10^2
2-5	-0.33	-0.39	-0.056	-6.7×10^1
3-8	-0.28	-0.066	0.22	2.6×10^1
5-7	-1.35	-0.89	0.46	1.3×10^3
4-6	-0.17	-0.12	0.042	2.0×10^0
4-8	-0.057	-0.16	-0.11	-3.3×10^0